A variant of human growth differentiation factor-9 that improves oocyte developmental competence

Received for publication, February 13, 2020, and in revised form, April 26, 2020 Published, Papers in Press, April 29, 2020, DOI 10.1074/jbc.RA120.013050

William A. Stocker[1,2,3], Kelly L. Walton[1,2], Dulama Richani[4], Karen L. Chan[1,2], Kiri H. Beilby[5], Bethany J. Finger[6], Mark P. Green[6], Robert B. Gilchrist[4], and Craig A. Harrison[1,2,*]

From the [1]Biomedicine Discovery Institute, [2]Department of Physiology, Monash University, Clayton, Victoria, Australia, [3]Department of Chemistry and Biotechnology, Swinburne University of Technology, Hawthorn, Victoria, Australia, [4]School of Women's and Children's Health, Discipline of Obstetrics and Gynaecology, University of New South Wales Sydney, NSW, Australia, [5]Department of Obstetrics and Gynaecology, Monash University, Clayton, Victoria, Australia, and [6]School of BioSciences, University of Melbourne, Melbourne, Victoria, Australia

Edited by John M. Denu

Growth differentiation factor-9 (GDF9) and bone morphogenetic protein-15 (BMP15) are co-expressed exclusively in oocytes throughout most of folliculogenesis and play central roles in controlling ovarian physiology. Although both growth factors exist as homodimers, recent evidence indicates that GDF9 and BMP15 can also heterodimerize to form the potent growth factor cumulin. Within the cumulin complex, BMP15 "activates" latent GDF9, enabling potent signaling in granulosa cells via type I receptors (*i.e.* activin receptor-like kinase-4/5 (ALK4/5)) and SMAD2/3 transcription factors. In the cumulin heterodimer, two distinct type I receptor interfaces are formed compared with homodimeric GDF9 and BMP15. Previous studies have highlighted the potential of cumulin to improve treatment of female infertility, but, as a noncovalent heterodimer, cumulin is difficult to produce and purify without contaminating GDF9 and BMP15 homodimers. In this study we addressed this challenge by focusing on the cumulin interface formed by the helix of the GDF9 chain and the fingers of the BMP15 chain. We demonstrate that unique BMP15 finger residues at this site (Arg^{301}, Gly^{304}, His^{307}, and Met^{369}) enable potent activation of the SMAD2/3 pathway. Incorporating these BMP15 residues into latent GDF9 generated a highly potent growth factor, called hereafter Super-GDF9. Super-GDF9 was >1000-fold more potent than WT human GDF9 and 4-fold more potent than cumulin in SMAD2/3-responsive transcriptional assays in granulosa cells. Our demonstration that Super-GDF9 can effectively promote mouse cumulus cell expansion and improve oocyte quality *in vitro* represents a potential solution to the current challenges of producing and purifying intact cumulin.

Growth differentiation factor-9 (GDF9) and bone morphogenetic protein-15 (BMP15) are oocyte-secreted members of the transforming growth factor-β (TGF-β) superfamily (1, 2). GDF9 and BMP15 are synthesized as precursor proteins, consisting of pro- and mature domains, with the prodomain templating the folding and dimerization of the mature growth factors (3, 4). Mature GDF9 activates Smad2/3 transcription factors via binding to complexes of type I (activin receptor-like kinase-5 (ALK5)) and type II (BMPRII) TGF-β family receptors (5, 6). BMP15 also utilizes BMPRII, but binds a distinct type I receptor (ALK6) and activates the Smad1/5/8 pathway (7).

During folliculogenesis, GDF9 and BMP15 signaling stimulates granulosa cell (GC) proliferation, whereas preventing follicle-stimulating hormone (FSH)-induced differentiation toward the mural GC phenotype (8, 9). In antral follicles, GDF9 and BMP15 direct GCs immediately surrounding the oocyte toward the specialized cumulus cell phenotype, which, in turn, facilitates oocyte maturation and the acquisition of developmental competence (10). In mice, *in vitro* studies have suggested that the above functions are primarily dependent upon activation of the GDF9-Smad2/3 axis (11, 12) and, in support, GDF9 knockout mice are infertile (13), whereas BMP15 knockout mice display only a mild reproductive phenotype (14). In monoovulatory species, however, both the GDF9-Smad2/3 axis and the BMP15-Smad1/5/8 axis appear to play prominent roles in GC function, with sheep homozygous for inactivating mutations in either GDF9 or BMP15 displaying infertility (15). Similarly in women, mutations in GDF9 and BMP15 have been identified in cases of primary ovarian insufficiency, polycystic ovary syndrome, and dizygotic twinning (16).

The species differences in GDF9 and BMP15 identified through genetic studies have been further elaborated by biochemical analysis of these unique TGF-β proteins (Table S2). For example, mouse GDF9 is produced in an active form, whereas human GDF9 is latent due to a high affinity interaction with its N-terminal prodomain, which blocks receptor binding (3, 17). Furthermore, human BMP15 is produced in an active form, whereas ovine BMP15 is inactive, and mouse BMP15 is misfolded and typically not secreted from cells (18).

The discrepancy between the genetic requirement for both GDF9 and BMP15 in monoovulatory species and the latency of recombinant human and ovine GDF9 (as well as ovine BMP15) was recently resolved by two separate groups through the generation of a highly bioactive human GDF9:BMP15 heterodimer, named cumulin (19, 20). Both groups showed that cumulin potently activates Smad2/3 signaling, stimulating cultured mouse GC to proliferate (19) and inducing genes required for cumulus cell expansion (20). Additionally, porcine cumulus-oocyte complexes (COCs) supplemented with recombinant human cumulin during *in vitro* maturation (IVM) better sup-

This article contains supporting information.

* For correspondence: Craig A. Harrison: craig.harrison@monash.edu.

ported embryo development to at least day 7, whereas human GDF9 and BMP15 homodimers provided no apparent benefit in this model (19). Together, these studies indicate that activation of latent human GDF9 is likely mediated through heterodimerization with BMP15, leading to potent Smad2/3 signaling (19, 20).

Based on its *in vitro* activity, cumulin has great potential as an IVM supplement to improve assisted reproductive technology (ART) (19). However, the structure of cumulin as a noncovalent heterodimer creates challenges during production and purification. Specifically, co-transfecting mammalian cells with both *GDF9* and *BMP15* cDNA results in production of cumulin, together with GDF9 and BMP15 homodimers. This approach has typically resulted in a BMP15 homodimer production bias, relative to cumulin (19, 20). To date, attempts to isolate cumulin free of contaminating homodimers has resulted in loss of activity on cumulus granulosa cells, likely due to prodomain separation during purification (19). To circumvent these issues, we sought to activate homodimeric human GDF9. Specific BMP15 residues predicted to activate GDF9 within the cumulin complex were substituted into the *GDF9* cDNA. The resultant Super-GDF9 protein was expressed at high levels and stimulated Smad2/3 signaling with at least 4-fold greater potency than cumulin itself.

Results

Smad signaling by human GDF9, BMP15, and cumulin

Following synthesis and proteolytic cleavage, GDF9, BMP15, and cumulin are secreted from cells noncovalently associated with their prodomains (Fig. 1*A*) (19). In this study, each of these proteins was produced in HEK-293T cells and Co-IMAC was used to purify the His-tagged pro-mature complexes. To assess activity, COV434 human GCs were transfected with Smad-responsive transcriptional reporters and treated overnight with increasing doses of GDF9, BMP15, or cumulin, all in their pro-forms. As expected, GDF9 induced no transcriptional activity at any of the doses tested (Fig. 1, *B* and *C*). In contrast, treatment with BMP15 dose-dependently stimulated the Smad1/5/8-responsive transcriptional reporter, leading to high levels of luciferase activity (Fig. 1*C*). BMP15 also induced a low level of Smad2/3-responsive transcriptional activity (Fig. 1*B*). Consistent with previous studies, cumulin dose-dependently stimulated the Smad2/3-responsive reporter and the Smad1/5/8-responsive reporter, leading to high levels of luciferase activity in both assays (Fig. 1, *B* and *C*). To support these transcriptional assays, we assessed Smad1/5 and Smad2 phosphorylation in COV434 cells stimulated for 1 h with GDF9, BMP15, or cumulin, all in their pro-forms. GDF9 failed to activate either Smad pathway (Fig. 1*D*). However, both BMP15 and cumulin stimulated phosphorylation of Smad1/5 and Smad2 (albeit to different extents) (Fig. 1*D*).

How does BMP15 activate latent GDF9 in the cumulin heterodimer?

The luciferase and Smad phosphorylation assays indicated that, within the cumulin structure, BMP15 activates GDF9, as previously hypothesized (19). To provide molecular insights into this activation mechanism, we used homology modeling to

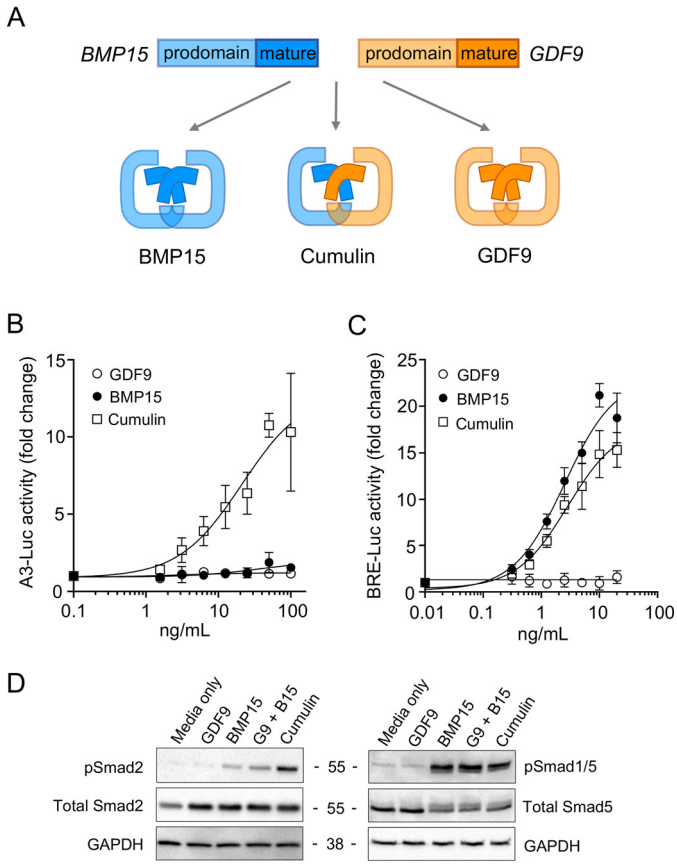

Figure 1. Smad signaling in response to human GDF9, BMP15, and cumulin. *A,* representation of human pro-GDF9, pro-BMP15, and pro-cumulin. *B* and *C,* dose-response curves in COV434 human GC transfected with (*B*) a Smad2/3-responsive luciferase reporter (A3-Luc; ligand concentrations 1.6 to 100 ng/ml), or (*C*) a Smad1/5/8-responsive luciferase reporter (BRE-Luc; ligand concentrations 0.3 to 20 ng/ml). Luciferase activity is presented as the mean ± S.D. of at least triplicates from representative experiments, relative to an adjusted value of 1.0 for the mean of the control wells. Experiments were repeated >3 times. *D,* COV434 cells were treated for 1 h (50 ng/ml). Phosphorylated Smad proteins were detected using anti-phospho-Smad2 or anti-phospho-Smad1/5. Anti-GAPDH, anti-Smad2, and anti-Smad5 were used as internal controls.

obtain a structural model of cumulin. Similar to the models of mature BMP15 and GDF9 (Fig. 2, *A* and *B*), cumulin displays the typical butterfly-shaped architecture of TGF-β superfamily ligands (Fig. 2*C*). Based on the crystal structures of TGF-β superfamily ligands bound to their type I and/or type II receptors (21–24), cumulin would interact with its type II receptor (BMPRII) in the "knuckle" region formed by its finger domains (Fig. 2*C*). Type I receptor (ALK4/5/6) binding, in contrast, would occur in the "wrist" regions of cumulin, which are formed by residues from both the BMP15 and GDF9 chains (Fig. 2*C*). As a heterodimer, two distinct type I receptor interfaces (wrist regions) are formed in cumulin, relative to homodimeric GDF9 and BMP15. In this study, we focused on the cumulin wrist epitope formed by the helix of the GDF9 chain (Fig. 2*C*, *gold*) and the fingers of the BMP15 chain (Fig. 2*C*, *cyan*). Unique BMP15 finger residues at this site likely enable high affinity ALK4/5 binding and activation of the Smad2/3 pathway, a process not achievable by the latent GDF9 homodimer. Sequence alignment of the finger domains of BMP15 and GDF9 identified 6 conservative and 10 nonconser-

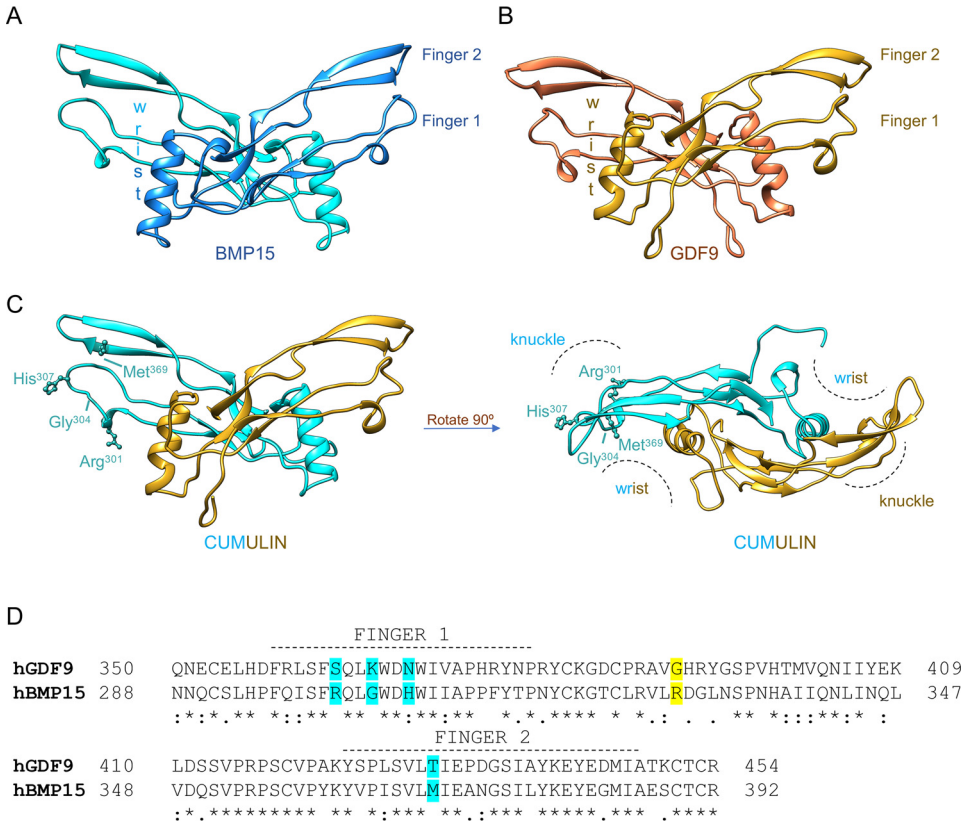

Figure 2. BMP15 activates latent GDF9. *A,* ribbon plot of human mature BMP15 showing the canonical dimer architecture. The two monomer subunits of the homodimer are colored *cyan* and *blue*. The putative binding epitopes for the type I receptors (*wrist* and *fingers*) are indicated. *B,* ribbon plot of human mature GDF9 showing the canonical dimer architecture. The two monomer subunits of the homodimer are colored in *gold* and *orange*. The putative binding epitopes for the type I receptors (*wrist* and *fingers*) are indicated. *C,* ribbon plot of human mature cumulin showing the canonical butterfly-shaped dimer architecture, and then rotated around the *x* axis by 90°. The monomer subunits of the heterodimer are colored in *cyan* (BMP15) and *gold* (GDF9). The putative binding epitopes for the type I (*wrist*) and type II (*knuckle*) receptors are indicated. Four BMP15 finger residues (Arg^{301}, Gly^{304}, His^{307}, and Met^{369}), which likely enable high affinity ALK4/5 binding are shown. *D,* sequence alignment of the mature domains of human GDF9 and BMP15 (excluding the disordered N terminus). The residues are numbered according to the first residue of the signal peptide. Residues forming the fingers are indicated. Residues modified in this study are highlighted in *cyan* (*fingers*) and *yellow* (*wrist*). Identical (*) and conserved (*dot* and *colon*) amino acid residues between GDF9 and BMP15 are indicated.

vative amino acid differences (Fig. 2*D*). Based on the ternary ligand-receptor complex of BMP2 (22), four of the identified BMP15 residues (Arg^{301}, Gly^{304}, His^{307}, and Met^{369}; Fig. 2*D*, *cyan*) are likely involved in type I receptor binding. The corresponding residues in latent human GDF9 are Ser^{363}, Lys^{366}, Asn^{369}, and Thr^{431}, respectively (Fig. 2*D*).

Generation and characterization of Super-GDF9

Using site-directed mutagenesis, we incorporated the identified BMP15 residues, in various combinations, into latent human GDF9. As it has previously been shown that substituting Gly^{391} in the pre-helix loop of human GDF9 to arginine (present in both mouse GDF9 and human BMP15) reduces latency (17, 25), we also included this change in our mutant panel (Table 1). The BMP15 residues were incorporated into both chains of the GDF9 homodimer. HEK-293T cells were transiently transfected with expression vectors for the GDF9 variants and the conditioned medium was subjected to Western blotting. Using a GDF9-targeted antibody (mAb-53/1), the monomeric mature (20 kDa) and precursor (60 kDa) forms of GDF9 were detected for each mutant (Fig. 3*A*), confirming they were secreted normally. Therefore, we carried out large-scale production of each variant and used Co-IMAC to purify the N terminally tagged pro-GDF9 complexes.

Table 1
Human GDF9 variants

Protein name	Mutations to human GDF9
$GDF9^{G391R}$	G391R
Mutant 1	K366G,N369H,G391R
Mutant 2	S363R,N369H,G391R
Mutant 3	S363R,K366G,G391R
Mutant 4	S363R,K366G,N369H,G391R
Super-GDF9	S363R,K366G,N369H,G391R,T431M

To assess activity, COV434 granulosa cells, transfected with Smad-responsive luciferase reporters, were treated with the purified pro-GDF9 variants. The base mutation (G391R) marginally activated human GDF9 in the Smad2/3-responsive assay (Fig. 3, *B* and *C*). Incorporating various combinations of BMP15 residues from finger 1 into human GDF9 led to a progressive increase in reporter activity. Specifically, mutant 2 (S363R, N369H,G391R), mutant 1 (K366G,N369H,G391R), and mutant 3 (S363R,K366G,G391R) were 3-, 11-, and 14-fold more potent, respectively, than the G391R variant alone (Fig. 3*B*). The high activity of mutants 1 and 3, relative to mutant 2, identified the K366G mutation as a key determinant for enhanced type I receptor binding. Surprisingly, incorporating all four of these BMP15 residues into human GDF9 (mutant 4: S363R,K366G,N369H,G391R) had a synergistic effect, dramatically increasing both potency (50-fold) and the maximal

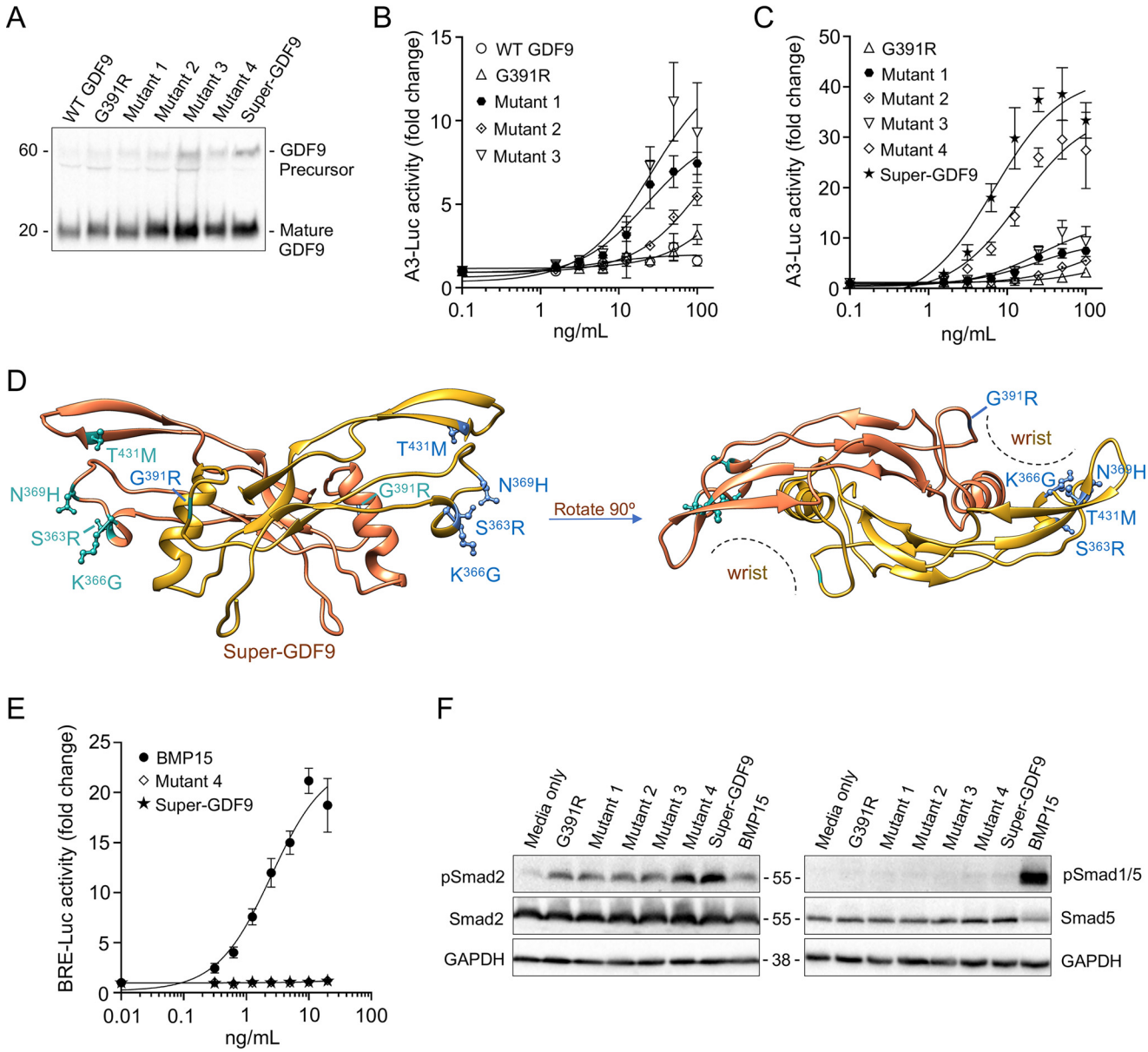

Figure 3. Generation and characterization of Super-GDF9. *A,* BMP15 residues were substituted into GDF9 using *in vitro* site-directed mutagenesis. Conditioned media from HEK-293T cells transfected with WT or mutant constructs were analyzed by Western blotting using mAb-53/1, targeted to the GDF9 mature domain. *B*, *C*, and *E,* dose-response curves in COV434 human GC transfected with (*B* and *C*) a Smad2/3-responsive luciferase reporter (A3-Luc; ligand concentrations 1.6 to 100 ng/ml). Note the difference in *y* axes scale between *B* and *C*, or *E,* a Smad1/5/8-responsive luciferase reporter (BRE-Luc; ligand concentrations 0.3 to 20 ng/ml). Luciferase activity is presented as the mean ± S.D. of at least triplicates from representative experiments, relative to an adjusted value of 1.0 for the mean of the control wells. Experiments were repeated >3 times. *D,* ribbon plot of mature Super-GDF9 showing the canonical butterfly-shaped dimer architecture, and then rotated around the *x* axis by 90°. The two monomer subunits of the homodimer are colored in *gold* and *orange*. The putative binding epitopes for the type I receptors (*wrist*) are indicated. Residues that were substituted to the corresponding residues in BMP15 are shown in *blue* (S363R,K366G,N369H,G391R,T431M). *F,* COV434 cells were treated for 1 h (50 ng/ml). Phosphorylated Smad proteins were detected using anti-phospho-Smad2 or anti-phospho-Smad1/5. Anti-GAPDH, anti-Smad2, and anti-Smad5 were used as internal controls.

response (Fig. 3*C*, note the difference in *y* axes scale between *B* and *C*). Finally, our modeling also identified a BMP15 residue from finger 2 (Met^{369}) that could potentially contribute to type I receptor binding. Incorporating this residue into mutant 4 generated a particularly potent GDF9 variant (Super-GDF9: S363R,K366G,N369H,G391R,T431M; Fig. 3*D*), which was >100-fold more potent than the G391R variant alone and induced a remarkable 40-fold increase in Smad2/3-responsive luciferase activity (Fig. 3*C*).

Incorporating five BMP15 residues activated latent human GDF9, enabling potent stimulation of the Smad2/3 pathway. Because BMP15 typically activates the alternative Smad1/5 pathway, we assessed whether the GDF9 variants might also activate these transcription factors. COV434 granulosa cells were transfected with a Smad1/5/8-responsive reporter and then treated with increasing doses of BMP15, GDF9 (mutant 4), or Super-GDF9. Only BMP15 induced a luciferase response in this Smad1/5/8 assay (Fig. 3*E*). Consistent with this, no Smad1/5 phosphorylation was detectable by Western blotting in cells treated with any of the GDF9 variants (Fig. 3*F*). Thus, Super-GDF9 and the other GDF9 variants only activated the Smad2/3 pathway. Finally, we examined how Super-GDF9 was

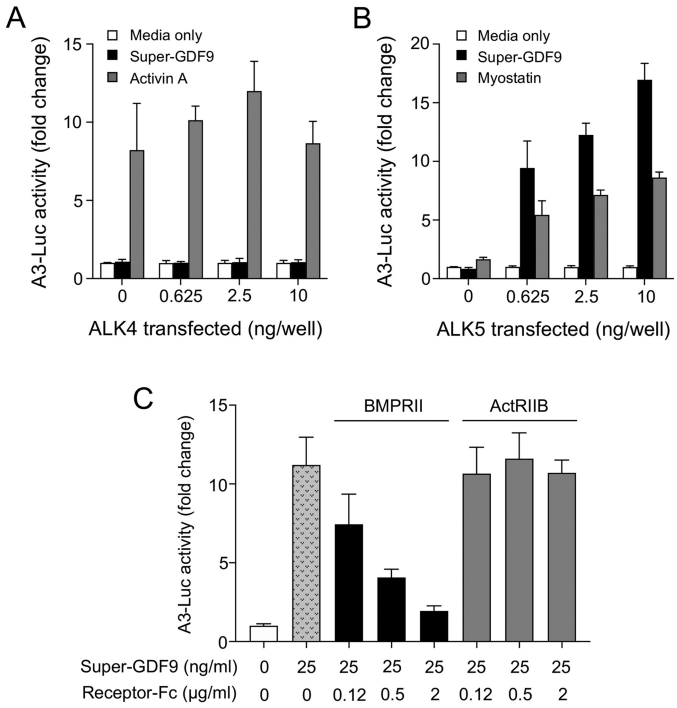

Figure 4. Super-GDF9 uses the type I receptor ALK5 and the type II receptor BMPRII. *A,* R1B L17 mink lung epithelial cells treated with Super-GDF9 (50 ng/ml) or activin A (5 ng/ml), 24 h after being transiently transfected with a Smad2/3-responsive luciferase reporter and increasing amounts (0–10 ng/well) of ALK4 expression vector. *B,* R1B L17 mink lung epithelial cells treated with Super-GDF9 (50 ng/ml) or myostatin (10 ng/ml), 24 h after being transiently transfected with a Smad2/3-responsive luciferase reporter and increasing amounts (0–10 ng/well) of ALK5 expression vector. Luciferase activity in *A* and *B,* is presented as the mean ± S.D. of at least triplicates from representative experiments, relative to an adjusted value of 1.0 for the mean of the control wells for each quantity of receptor. *C,* COV434 human granulosa cells transfected with a Smad2/3-responsive luciferase reporter were treated with Super-GDF9 alone, or Super-GDF9 together with increasing concentrations of either BMPRII-ECD-Fc or ActRIIB-ECD-Fc. Luciferase activity is presented as the mean ± S.D. of at least triplicates from representative experiments, relative to an adjusted value of 1.0 for the mean of the control wells.

able to induce such a potent transcriptional response, relative to GDF9^{G391R} (Fig. 3*C*), despite both proteins promoting Smad2 phosphorylation following 1 h of treatment (Fig. 3*F*). Time course analysis demonstrated the capacity of Super-GDF9 to sustain a high level of Smad2 phosphorylation for an extended period of time, relative to GDF9^{G391R} (Fig. S1).

Defining Super-GDF9 receptor preference

To determine which type I receptor Super-GDF9 signals through, we utilized R1B L17 cells, which express no ALK5 and very low levels of ALK4 (26–29). R1B L17 cells, co-transfected with a Smad2/3-responsive luciferase reporter and an expression vector for either ALK4 or ALK5, were treated with media alone, activin A, myostatin, or Super-GDF9 (Fig. 4, *A* and *B*). Although activin A induced a robust luciferase response in cells transfected with ALK4 (28–30), Super-GDF9 had no effect (Fig. 4*A*). In contrast, Super-GDF9 potently activated the luciferase reporter in cells transfected with ALK5 (Fig. 4*B*). Indeed, Super-GDF9 induced a greater luciferase response than the positive control, myostatin (31, 32), in this assay. Thus, Super-GDF9 activates Smad2/3 signaling via ALK5, but not via ALK4.

Next, we assessed the capacity of exogenous type II receptor extracellular domains (ECD) to antagonize the activity of Super-GDF9 on COV434 granulosa cells transfected with a Smad2/3-responsive luciferase reporter (Fig. 4*C*). When used alone, Super-GDF9 stimulated high levels of luciferase activity. Co-treatment with BMPRII-ECD, fused to an IgG Fc domain for stability, antagonized Super-GDF9 activity in a dose-dependent manner. In contrast, addition of activin receptor type IIB (ActRIIB) ECD-Fc had no effect on Super-GDF9 activity (Fig. 4*C*). Thus, BMPRII is the type II receptor for Super-GDF9.

Super-GDF9 stimulates granulosa cell functions with greater potency than cumulin

To assess whether Super-GDF9 works as effectively as cumulin, we initially compared the purified proteins in the COV434 Smad2/3-responsive luciferase assay (Fig. 5*A*). In this assay, Super-GDF9 was ~4-fold more potent than cumulin and stimulated a higher maximum response. One of the physiological functions of oocyte-secreted factors (OSFs) on GCs is to drive development of the cumulus cell phenotype (33, 34). During the peri-ovulatory period, cumulus cells undergo a highly coordinated process, known as cumulus expansion, where they produce a complex extracellular matrix (ECM) critical to successful ovulation and fertilization (35). Critical genes involved with ECM production and stability during cumulus expansion (*Ptx3*, *Has2*, and *Ptgs2*) are downstream targets of mouse GDF9, human BMP15, and cumulin (19, 20). Therefore, we assessed whether Super-GDF9 could stimulate expression of *Ptx3*, *Has2*, and *Ptgs2* in cultured mouse GC (Fig. 5, *B–D*). In agreement with the response in the luciferase assay (Fig. 5*A*), Super-GDF9 was ~5-fold more potent than cumulin in terms of inducing *Ptx3* and *Has2* expression (Fig. 5, *B* and *C*), whereas *Ptgs2* expression was similarly regulated by both growth factors (Fig. 5*D*).

Super-GDF9 improves oocyte developmental competence

To characterize Super-GDF9 and cumulin in a model closer to the physiological role of OSFs, we assessed whether treatment of isolated mouse cumulus-oocyte complexes during IVM could enhance cumulus expansion. At 50 ng/ml, both Super-GDF9 and cumulin significantly improved cumulus expansion after 17 h of IVM (Fig. 5*E*). To investigate whether these effects on cumulus cells also translated to an improvement in oocyte developmental competence, the oocytes were subsequently fertilized and their capacity to support embryo development to the blastocyst stage was assessed (Fig. 5*F*). Relative to untreated controls, oocytes matured in the presence of 50 ng/ml of Super-GDF9 or cumulin showed significantly improved blastocyst development rates at 5 days post-fertilization.

Discussion

The major role of the oocyte-specific growth factors GDF9 and BMP15 is to regulate the growth and differentiation of GCs, which in turn supply the oocyte with the support necessary for future healthy embryo/fetal development (10, 36–39). Human BMP15 binds to complexes of type I (ALK6) and type II (BMPRII) receptors on the surface of GCs (Fig. 6*A*) and leads to the activation of Smad1/5 transcription factors (7). In contrast, human GDF9 remains associated with

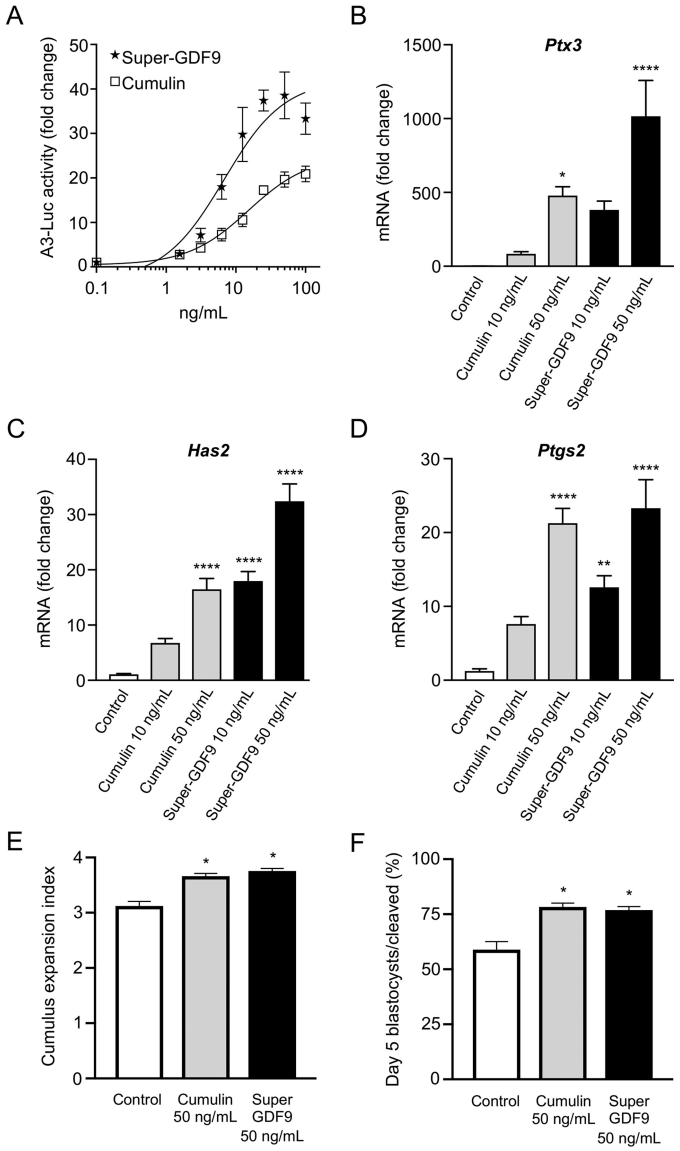

Figure 5. Super-GDF9 *versus* pro-cumulin. *A,* dose-response curves in COV434 human GC transfected with a Smad2/3-responsive luciferase reporter (A3-Luc; ligand concentrations 1.6 to 100 ng/ml). Primary mouse GC mRNA expression of (*B*) *Ptx3*, (*C*) *Has2*, and (*D*) *Ptgs2* relative to media-only controls measured by qPCR. *E,* morphological cumulus expansion of mouse COCs scored after 17 h of IVM using the Vanderhyden criteria. *F,* effects of the treatments on mouse oocyte developmental competence after 17 h of IVM assessed as the day 5 blastocyst rate as a percentage of the number of cleaved embryos. Data in *A* are presented as the mean ± S.D. of at least triplicates from representative experiments, relative to an adjusted value of 1.0 for the mean of the control wells. Experiments were repeated >3 times. *B–D,* data are presented as the mean ± S.E. ($n = 7$). *E* and *F,* data are presented as the mean ± S.E., from 104 to 130 COCs per treatment across three biological repetitions. *, $p < 0.05$; **, $p < 0.01$; ****, $p < 0.0001$ compared with media-only controls.

its prodomain in a latent complex (Fig. 6*A*) (3). Even following prodomain removal, mature hGDF9 has very low signaling capacity via Smad2/3 transcription factors (17). For many years the latency of human GDF9 was a major conundrum in the field, as many of the important actions of these growth factors on GCs are dependent upon Smad2/3 activation (11, 12, 20, 40). Then, two groups discovered that GDF9 and BMP15 readily form a heterodimer, termed cumulin (19, 20), which binds two distinct type I receptors (ALK4/5 and ALK6) and potently activates both Smad2/3 and Smad1/5 transcription pathways (Fig. 6*A*).

In this study, we sought to understand the molecular mechanisms underlying the potent Smad2/3-activating capacity of cumulin, relative to latent human GDF9. One possible mechanism could be that the conformation of cumulin differs from latent GDF9 homodimers in a way that allows the α-helix region of the GDF9 chain to bind ALK4/5 with much higher affinity. A second possible mechanism is that cumulin may be in a conformation that limits the inhibitory effect of the GDF9 prodomain, as has been discussed previously by Peng and colleagues (25). A third possible mechanism is that BMP15 finger residues directly bind ALK4/5 with high affinity. Although we cannot rule out a reduction in the inhibitory effect of the GDF9 prodomain as being a contributing factor toward the enhanced activity of cumulin, our development of Super-GDF9 suggests direct binding by BMP15 finger residues is likely to be the most crucial factor. As described previously (19), type I receptor-binding epitopes are distinct in cumulin, relative to GDF9 and BMP15 (type II receptor-binding sites, in contrast, are maintained across the three proteins). One of these unique epitopes, formed by the α-helix of the GDF9 chain and residues on the convex surface of the fingers of the BMP15 chain, was identified as the most likely ALK4/5 receptor-binding site. As the α-helix at this site is common to both cumulin and latent GDF9, we reasoned that enhanced signaling capacity via Smad2/3 must be conveyed by BMP15 finger residues. In particular, modeling identified three finger 1 residues (Arg^{301}, Gly^{304}, and His^{307}) and one finger 2 residue (Met^{369}) within BMP15 distinct from the corresponding residues in GDF9. Arg^{301}, Gly^{304}, and His^{307} form a contiguous interface on the fingertip of the BMP15 chain, and the corresponding residues on BMP2 (22, 41) and GDF5 (21) have been implicated in type I receptor binding. In addition, residues in BMP2, GDF11, and GDF5, analogous to Met^{369} in BMP15, interact with their respective type I receptors (21, 22, 42). Introducing these four BMP15 residues, together with Arg^{329} (18), into latent GDF9 generated a novel, highly potent growth factor, which we termed Super-GDF9. Super-GDF9 was >1000-fold more potent than WT human GDF9 and >100-fold more active than $GDF9^{G391R}$, which was the most active human GDF9 homodimer previously described (17, 25). Moreover, Super-GDF9 even displayed a greater maximal Smad2/3 response than cumulin, likely because the BMP15 residues were incorporated into both chains of the GDF9 homodimer, forming two high affinity ALK5-binding sites. Our results support the idea that *in vivo* activation of latent hGDF9 occurs via heterodimerization with BMP15 (19), but also indicate that hGDF9 can be activated *in vitro* by the introduction of specific BMP15 residues.

In response to the luteinizing hormone surge, cumulus GCs immediately surrounding the oocyte expand and produce a thick extracellular matrix, which is critical for ovulation, fertilization, and ensuing embryo development (10, 35). Peng and colleagues (20) showed that cumulin, via Smad2/3, potently induced the expression of "expansion" genes (*Ptx3*, *Has2*, and *Ptgs2*) in GCs, as well as the full process of expansion in mouse oocytectomized cumulus cell complexes. Subsequently, we demonstrated that porcine cumulus-oocyte complexes supple-

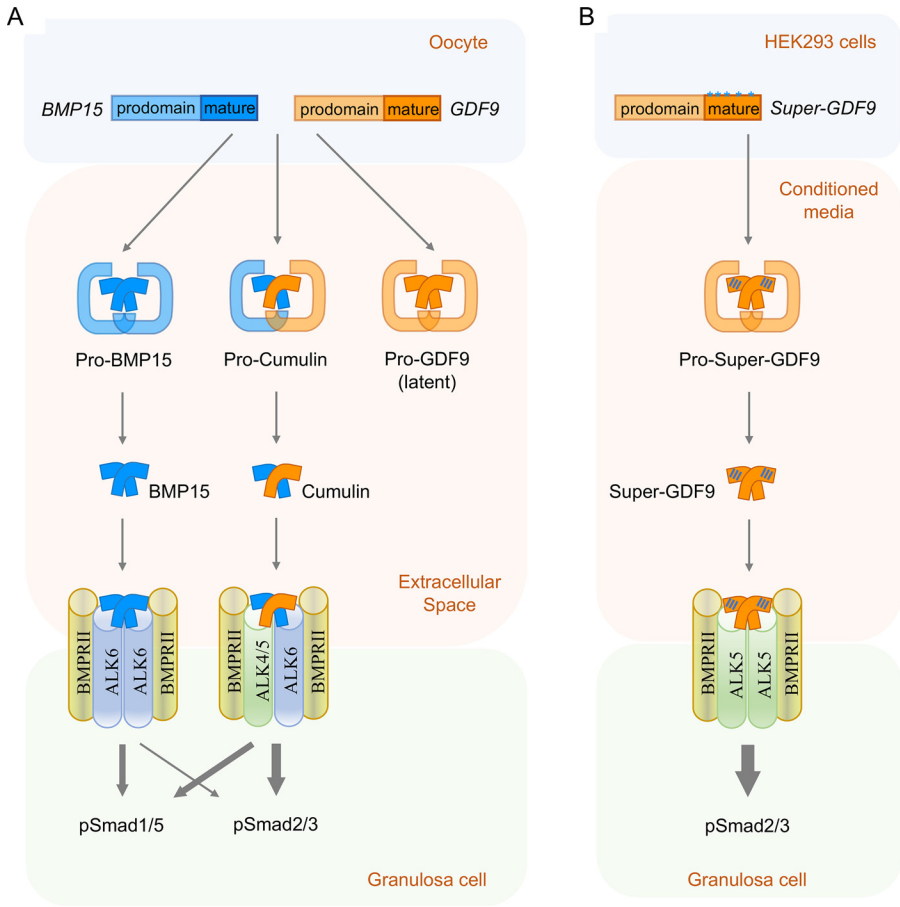

Figure 6. Model of human BMP15, GDF9, cumulin, and Super-GDF9 formation and signaling. *A, BMP15* and *GDF9* are co-expressed in mammalian oocytes throughout most of folliculogenesis. During synthesis, their prodomains direct the folding and dimerization of their mature domains. Dimeric precursors are cleaved by furin-like proteases, and then BMP15, GDF9, and potentially cumulin are secreted from the oocyte noncovalently associated with their prodomains. Following prodomain displacement in the extracellular matrix of nearby granulosa cells, BMP15 binds two BMPRII receptors and two ALK6 receptors to signal predominantly via pSmad1/5, but also weakly via pSmad2/3. Cumulin forms a receptor complex consisting of two BMPRII receptors, one ALK6 receptor, and one ALK4/5 receptor to signal via both Smad pathways, with pSmad2/3 signaling essential for many of its principal functions. Human GDF9 is naturally latent due to a high affinity interaction with its prodomain that prevents receptor binding. *B, Super-GDF9* can be expressed in transfected HEK293 cells. During synthesis, its prodomain directs the folding and dimerization of the mature domains. Dimeric precursors are likely cleaved by furin-like proteases and it is then secreted noncovalently associated with its prodomain. Following purification, when pro-Super-GDF9 is added to the media of cultured granulosa cells the prodomain is hypothetically displaced in the extracellular matrix. Super-GDF9 then binds two BMPRII receptors and two ALK5 receptors to potently signal via pSmad2/3.

mented with recombinant human cumulin during *in vitro* maturation are better able to support embryo development to at least day 7 (19). These studies highlighted the significant potential of cumulin to promote oocyte developmental competence *in vitro* and, thereby, impact human clinical IVM and advanced breeding in domestic animals. However, as a noncovalent heterodimer, cumulin is difficult to produce and purify free of contaminating GDF9 and BMP15 homodimers. Our development of Super-GDF9, a homodimer with potent Smad2/3-activating capacity, represents a potential solution to the problems surrounding cumulin production and purification.

In support, we showed that Super-GDF9 was 4- to 5-fold more potent than cumulin in activating the Smad2/3 pathway and stimulating the expression of the cumulus expansion genes *Ptx3* and *Has2* (*Ptgs2* expression was similarly regulated by both growth factors). Of importance for human ART, cumulus cells from oocytes that develop into better quality embryos display stronger expression of *HAS2* and *PTGS2* (43–45). Importantly, Super-GDF9 was as effective as cumulin at promoting cumulus cell expansion and improving mouse oocyte developmental competence. These results provide support for the concept that Smad2/3 activation, without Smad1/5 activation, is sufficient to drive the specialized cumulus cell functions that facilitate mouse oocyte maturation and the acquisition of developmental competence (20). Thus, Super-GDF9 may be an effective substitute for cumulin to improve the efficiency of IVM and make this procedure more clinically viable.

Although the *in vitro* results for Super-GDF9 are highly encouraging, this protein differs from cumulin in one key aspect: it cannot activate the Smad1/5 pathway. This distinction may be important, because Smad1/5 activation during bovine IVM may contribute to oocyte maturation and subsequent embryo development (37, 38). Critically, with the generation of Super-GDF9, we now have the tools to address this question. Indeed, future experiments will compare the effects on oocyte maturation and embryo development of Super-GDF9 alone, or in combination with BMP15.

In summary, the engineering of Super-GDF9 has uncovered the underlying biochemical basis for cumulin's substantial bioactivity. To date, Super-GDF9 has been shown to replicate the

biological functions of cumulin and, thus, this protein may provide an expeditious approach toward generating a potent recombinant OSF of clinical-grade purity for use as an IVM supplement.

Experimental procedures

Production of GDF9/BMP15 variants

Construction of the human (h) GDF9 and BMP15 expression vectors has been described previously (19). The hGDF9 cDNA was amplified by PCR and subcloned into the mammalian expression vector pCDNA3.1(+) (Thermo Fisher Scientific, Waltham, MA, United States) between the restriction sites NheI and EcoRI. For activation of hGDF9, multiple point mutations were incorporated into the cDNA using mutagenic primers (Table S1) with the QuikChange Lightning Multi Site-directed Mutagenesis Kit (Agilent Technologies, Santa Clara, CA, United States).

For production of recombinant human GDF9, BMP15, and cumulin, HEK-293T cells were plated at 8×10^5 cells/well in 6-well-plates in Dulbecco's modified Eagle's medium (DMEM) supplemented with 10% fetal calf serum (FCS) and incubated at 37 °C in 5% CO_2. After overnight incubation, plasmid DNA (2.5 μg/construct) was combined with polyethylenimine-MAX (Polysciences, Warrington, PA, United States) and after 10 min DNA-polyethylenimine complexes were added directly to cells and incubated in Opti-MEM (Life Technologies, United States) medium for 4 h before replacing with fresh Opti-MEM for 16 h. The medium was then replaced with production media (DMEM:F-12 medium containing GlutaMAX^{TM} (Life Technologies, United States), 0.02% bovine serum albumin (BSA), 0.005% heparin (Sigma, United States)) and incubated a further 72 h before collection.

Conditioned media was concentrated 5-fold with Nanosep microconcentrators (10 kDa molecular mass cut-off; Pall Life Sciences, Port Washington, NY, United States) before separation of reduced samples by 10% SDS-PAGE and Western blotting. The primary antibodies (used at a 1:5,000 dilution) targeting GDF9 (mAb-53/1) and BMP15 (mAb-28A) were from Oxford Brookes University (Oxford, UK) (4, 46). The secondary antibody (diluted 1:10,000) was horseradish peroxidase-conjugated anti-mouse IgG (GE Healthcare, Buckinghamshire, UK), with detection of immunoreactive proteins using Lumi-light chemiluminescence reagents (Roche, Basel, Switzerland) and a ChemiDoc^{TM} (Bio-Rad).

Purification of GDF9/BMP15 variants

Conditioned media from HEK-293T cells transfected with cDNAs for GDF9 variants (~200 ml) was concentrated (Centricon Plus-70, 5 kDa molecular mass cut-off; Millipore, Billerica, MA, United States) and resuspended in binding buffer (50 mM phosphate buffer, 300 mM NaCl, pH 7.4) to a final volume of 5 ml. The concentrated media was subjected to purification by Co-IMAC as previously described (47). Bound proteins were eluted from the resin with elution buffer (50 mM phosphate buffer, 300 mM NaCl, 500 mM imidazole) and imidazole was removed from the preparation by dialysis against binding buffer using a Slide-A-Lyzer® MINI Dialysis Device (2 ml 3.5 K molecular mass cut-off; Thermo Fisher Scientific, United States). Mass estimates for GDF9, BMP15, and cumulin were determined by Western blotting using recombinant hGDF9 or hBMP15 mature proteins (R&D Systems, Minneapolis, MN, United States) as standards. Densitometry was assessed with Image Lab^{TM} software (Bio-Rad).

In vitro COV434 granulosa cell bioassays

COV434 human granulosa tumor cells (7.5×10^4 cells/well) were plated in DMEM, 10% FCS into 48-well-plates at 37 °C in 5% CO_2. The following day, cells were transfected using Lipofectamine 3000 (Life Technologies) with 250 ng/well of plasmid DNA. For the Smad2/3-responsive A3-luciferase assay, this consisted of 50 ng/well of pA3-Lux, 100 ng/well of pFAST2, and 100 ng/well of pCDNA3.1. For the Smad1/5/8-responsive BRE-luciferase assay, 250 ng/well of pBRE-Luc was transfected. The following day, cells were treated with increasing doses of GDF9/BMP15 variants diluted in low-serum media (DMEM with 50 mM HEPES and 0.2% FCS) and incubated overnight at 37 °C in 5% CO_2. The media was then removed and cells were lysed in solubilization buffer (26 mM glycylglycine (pH 7.8), 16 mM $MgSO_4$, 4 mM EGTA, 900 μM DTT, 1% Triton X-100). The lysate was transferred to a white 96-well-plate and luminescence was measured immediately after the addition of the substrate D-luciferin (Life Technologies) (48). To determine which type II receptor Super-GDF9 utilized, Fc-fused extracellular domains of BMPRII and ActRIIB (R&D Systems) were used to antagonize Super-GDF9 activity.

As an additional method of assessing activity, COV434 cells (10^6 cells/well in 6-well-plates) were treated with GDF9, BMP15, or cumulin (diluted in fresh low serum media) for 1 h at 37 °C in 5% CO_2 before lysis on ice in 70 μl of RIPA buffer (50 mM Tris base, 1% Nonidet P-40, 0.5% deoxycholic acid, 0.1% SDS, and 0.9% saline, pH 8.0) supplemented with phosphatase inhibitors (PhosSTOP, Roche) and protease inhibitors (Protease Inhibitor Mixture Set III, EDTA-Free; Calbiochem, Alexandria, Australia). Lysates were subjected to Western blotting before probing with anti-phospho-Smad2 or anti-phospho-Smad1/5 antibodies, followed by secondary anti-rabbit horseradish peroxidase-conjugated goat-IgG. For internal controls anti-GAPDH horseradish peroxidase-conjugated IgG was used, as well as anti-Smad2 (detects total Smad2) or anti-Smad5 (detects total Smad5). Antibodies were from Cell Signaling Technology (Danvers, MA). Primary antibodies were used at a 1:2,000 dilution and the secondary antibody was used at a 1:10,000 dilution.

Molecular modeling

The GDF9, BMP15, and cumulin structural models were created using the Swiss model comparative protein modeling server (49, 50) and the crystal structure of GDF5 (Protein Data Bank entry 1WAQ) as a template (51). Subsequently the UCSF Chimera package from the Resource for Biocomputing, Visualization, and Informatics at the University of California, San Francisco (52), was used to overlay the GDF9, BMP15, and cumulin dimers onto the GDF5 template and to produce the molecular graphics images.

Type I receptor utilization assays

R1B L17 mink lung epithelial cells (6×10^4 cells/well) were plated in DMEM, 10% FCS into 48-well-plates at 37 °C in 5% CO_2. The following day, cells were transfected using Lipofectamine 3000 with 250 ng/well of plasmid DNA, consisting of: 50 ng/well of pA3-Lux; 100 ng/well of pFAST2; 0 to 10 ng/well of ALK4 expression vector, or 0 to 10 ng/well of ALK5 expression vector; and 90 to 100 ng/well of empty pCDNA3.1 vector to normalize the total quantity of DNA transfected. After 24 h, transfected cells were treated with Super-GDF9, activin A, or myostatin (both from R&D Systems) diluted in low-serum media, and incubated overnight at 37 °C in 5% CO_2. The media was then removed and cells were lysed in solubilization buffer. The lysate was transferred to a white 96-well-plate and luminescence was measured immediately after the addition of the substrate D-luciferin.

Isolation and culture of primary mouse GC

Young female mice (129/T2/Sv, 21–28 days old) were primed with 5 IU pregnant mare's serum gonadotropin (PMSG) by intraperitoneal injection and ovaries were collected 46 h later. Mice were maintained in accordance with the Australian Code for the Care and Use of Animals for Scientific Purposes and with the approval of the Monash University Animal Ethics Committee. Antral follicles were punctured with a 27-gauge needle releasing GC into collection media (Medium-199 containing GlutaMAX™ (Life Technologies) + 3 mg/ml of BSA (Sigma-Aldrich) + 1% antibiotic-antimycotic (Life Technologies) + 25 mM HEPES). The GC pool was subsequently filtered using a 40-μm nylon cell strainer (Falcon®, Corning Inc., Corning, NY, United States) to remove oocytes. GC were plated at 10^6 cells/well in 24-well plates in media supplemented with 10% FCS. After overnight culture at 37 °C with 5% CO_2, media was removed and GC was treated with Super-GDF9 or cumulin (diluted in fresh serum-free media) for 6 h at 37 °C in 5% CO_2. Media was then removed and the plate was snap frozen and stored at −80 °C prior to RNA extraction.

Reverse-transcription PCR (RT-PCR)

RNA was extracted from GC using a GenElute™ Total RNA Purification Kit (Sigma-Aldrich) and subsequently subjected to DNase treatment with a TURBO DNA-*free*™ Kit (Thermo Fisher Scientific). Total RNA (500 ng) was then reverse transcribed to cDNA in a 20-μl reaction using random hexamers with the SuperScript® III First-Strand Synthesis System for RT-PCR (Life Technologies) on a T100™ Thermal Cycler (Bio-Rad). In 10 μl of quantitative PCR (qPCR) reactions, 1 μl of cDNA was used as template, carried out on a Mastercycler® epgradient *realplex*^{4} S (Eppendorf, Hamburg, Germany) using TaqMan™ Fast Universal PCR Master Mix (2 times), no AmpErase™ UNG (Thermo Fisher Scientific) and TaqMan™ Gene Expression assays (*Ptx3* Mm00477267_g1; *Has2* Mm00515089_m1; *Ptgs2* Mm00478374_m1). Each qPCR was carried out in duplicate and normalized to the housekeeping gene *Gapdh* (Mm99999915_g1). Relative mRNA levels were determined using the $2^{-\Delta\Delta CT}$ method (53, 54).

Oocyte quality assay

IVM and embryo cultures were performed as previously described (55) with minor modifications. Briefly, 28-day-old C57/Bl6 female mice were given 5 IU PMSG intraperitoneal injection. Mice were killed by cervical dislocation 46 h post-PMSG and ovaries were harvested. Mice were maintained in accordance with the Australian Code for the Care and Use of Animals for Scientific Purposes and with the approval of the University of New South Wales Animal Ethics Committee. Large antral follicles were punctured in HEPES-buffered αMEM medium containing 3 mg/ml of BSA (CellMaxx, MP Biomedicals, New Zealand) and 100 μM 3-isobutyl-1-methylxanthine to liberate COCs. COCs were washed with culture medium (bicarbonate-buffered αMEM containing 3 mg/ml of BSA, 1 mg/ml of fetuin (Sigma-Aldrich), and 50 ng/ml each of recombinant mouse amphiregulin and epiregulin (R&D Systems)) and matured in this culture medium ± 50 ng/ml Super-GDF9 or cumulin for 17 h at 37 °C with 5% CO_2 in air. Following 17 h of IVM, cumulus expansion was scored blinded using criteria described by Vanderhyden and colleagues (56).

For embryo production, all media were purchased from IVF Vet Solutions (Adelaide, Australia). Following IVM as described above, COCs were washed (Research Wash, supplemented with 4 mg/ml of BSA) and co-incubated with capacitated sperm for 3.5 h at 37 °C with 5% O_2, 6% CO_2, and 89% N_2 in fertilization medium (Research Fert) supplemented with 4 mg/ml of BSA. Sperm were recovered from hybrid CBB6F1 male mice >12 weeks of age. Presumptive zygotes were washed three times in wash medium and then once in cleavage medium (Research Cleave) supplemented with 4 mg/ml of BSA and cultured in cleavage medium drops overlayered with mineral oil at a density of one embryo per 2 μl of medium. Embryo development was assessed every 24 h over 6 days.

Statistical analysis

For gene expression assays, data were assessed with ordinary one-way analysis of variance then Tukey's multiple comparisons test. Cumulus expansion scores were assessed with a Kruskal-Wallis test followed by Dunn's multiple comparisons test. Blastocyst development data were arcsine transformed and then assessed using one-way analysis of variance followed by Tukey's multiple comparison's test. $p < 0.05$ was considered statistically significant.

Data availability

All data are contained within the manuscript.

Acknowledgments—We thank Dr. David Mottershead (Keele University, United Kingdom) for providing the GDF9 and BMP15 expression vectors and Lesley Ritter (The University of Adelaide, Australia) for providing advice about the culture of mouse granulosa cells. The Resource for Biocomputing, Visualization, and Informatics at the University of California, San Francisco, CA, was supported by National Institutes of Health Grant P41 RR-01081.

Author contributions—W. A. S., K. L. W., R. B. G., and C. A. H. conceptualization; W. A. S., D. R., K. H. B., B. J. F., and C. A. H. formal analysis; W. A. S., D. R., K. L. C., K. H. B., B. J. F., and M. P. G. inves-

tigation; W. A. S., D. R., K. L. C., and M. P. G. methodology; W. A. S. and C. A. H. writing-original draft; K. L. W., M. P. G., and R. B. G. supervision; K. L. W. project administration; K. L. W., R. B. G., and C. A. H. writing-review and editing; K. L. C. data curation; C. A. H. funding acquisition.

Funding and additional information—This work was supported by National Health and Medical Research Council (NHMRC) of Australia Grant 1121504), NHMRC Senior Research Fellowship 1117538 (to R. B. G.), and a Australian Government Research Training Program Stipend scholarship (to W. A. S.).

Conflict of interest—The authors declare that they have no conflicts of interest with the contents of this article.

Abbreviations—The abbreviations used are: GDF9, growth differentiation factor-9; BMP15, bone morphogenetic protein-15; TGF-β, transforming growth factor-β; ALK, activin receptor-like kinase; BMPRII, bone morphogenetic protein receptor type II; GC, granulosa cell; COC, cumulus-oocyte complex; IVM, oocyte *in vitro* maturation; ART, assisted reproductive technology; OSFs, oocyte-secreted factors; ECM, extracellular matrix; Co-IMAC, cobalt-based immobilized metal affinity chromatography; ECD, extracellular domain; PMSG, pregnant mare's serum gonadotropin; qPCR, quantitative PCR; DMEM, Dulbecco's modified Eagle's medium; FCS, fetal calf serum; GAPDH, glyceraldehyde-3-phosphate dehydrogenase.

References

1. McGrath, S. A., Esquela, A. F., and Lee, S. J. (1995) Oocyte-specific expression of growth-differentiation factor-IX. *Mol. Endocrinol.* **9,** 131–136 CrossRef Medline
2. Dube, J. L., Wang, P., Elvin, J., Lyons, K. M., Celeste, A. J., and Matzuk, M. M. (1998) The bone morphogenetic protein 15 gene is X-linked and expressed in oocytes. *Mol. Endocrinol.* **12,** 1809–1817 CrossRef Medline
3. Mottershead, D. G., Pulkki, M. M., Muggalla, P., Pasternack, A., Tolonen, M., Myllymaa, S., Korchynskyi, O., Nishi, Y., Yanase, T., Lun, S., Juengel, J. L., Laitinen, M., and Ritvos, O. (2008) Characterization of recombinant human growth differentiation factor-9 signaling in ovarian granulosa cells. *Mol. Cell Endocrinol.* **283,** 58–67 CrossRef Medline
4. Pulkki, M. M., Myllymaa, S., Pasternack, A., Lun, S., Ludlow, H., Al-Qahtani, A., Korchynskyi, O., Groome, N., Juengel, J. L., Kalkkinen, N., Laitinen, M., Ritovs, O., and Mottershead, D. G. (2011) The bioactivity of human bone morphogenetic protein-15 is sensitive to C-terminal modification: characterization of the purified untagged processed mature region. *Mol. Cell Endocrinol.* **332,** 106–115 CrossRef Medline
5. Vitt, U. A., Mazerbourg, S., Klein, C., and Hsueh, A. J. (2002) Bone morphogenetic protein receptor type II is a receptor for growth differentiation factor-9. *Biol. Reprod.* **67,** 473–480 CrossRef Medline
6. Mazerbourg, S., Klein, C., Roh, J., Kaivo-Oja, N., Mottershead, D. G., Korchynskyi, O., Ritvos, O., and Hsueh, A. J. (2004) Growth differentiation factor-9 signaling is mediated by the type I receptor, activin receptor-like kinase 5. *Mol. Endocrinol.* **18,** 653–665 CrossRef Medline
7. Moore, R. K., Otsuka, F., and Shimasaki, S. (2003) Molecular basis of bone morphogenetic protein-15 signaling in granulosa cells. *J. Biol. Chem.* **278,** 304–310 CrossRef Medline
8. Vitt, U. A., Hayashi, M., Klein, C., and Hsueh, A. J. (2000) Growth differentiation factor-9 stimulates proliferation but suppresses the follicle-stimulating hormone-induced differentiation of cultured granulosa cells from small antral and preovulatory rat follicles. *Biol. Reprod.* **62,** 370–377 CrossRef Medline
9. Otsuka, F., Yao, Z., Lee, T., Yamamoto, S., Erickson, G. F., and Shimasaki, S. (2000) Bone morphogenetic protein-15: identification of target cells and biological functions. *J. Biol. Chem.* **275,** 39523–39528 CrossRef Medline
10. Gilchrist, R. B., Lane, M., and Thompson, J. G. (2008) Oocyte-secreted factors: regulators of cumulus cell function and oocyte quality. *Hum. Reprod. Update* **14,** 159–177 CrossRef Medline
11. Gilchrist, R. B., Ritter, L. J., Myllymaa, S., Kaivo-Oja, N., Dragovic, R. A., Hickey, T. E., Ritvos, O., and Mottershead, D. G. (2006) Molecular basis of oocyte-paracrine signalling that promotes granulosa cell proliferation. *J. Cell Sci.* **119,** 3811–3821 CrossRef Medline
12. Dragovic, R. A., Ritter, L. J., Schulz, S. J., Amato, F., Thompson, J. G., Armstrong, D. T., and Gilchrist, R. B. (2007) Oocyte-secreted factor activation of SMAD 2/3 signaling enables initiation of mouse cumulus cell expansion. *Biol. Reprod.* **76,** 848–857 CrossRef Medline
13. Dong, J., Albertini, D. F., Nishimori, K., Kumar, T. R., Lu, N., and Matzuk, M. M. (1996) Growth differentiation factor-9 is required during early ovarian folliculogenesis. *Nature* **383,** 531–535 CrossRef Medline
14. Yan, C., Wang, P., DeMayo, J., DeMayo, F. J., Elvin, J. A., Carino, C., Prasad, S. V., Skinner, S. S., Dunbar, B. S., Dube, J. L., Celeste, A. J., and Matzuk, M. M. (2001) Synergistic roles of bone morphogenetic protein 15 and growth differentiation factor 9 in ovarian function. *Mol. Endocrinol.* **15,** 854–866 CrossRef Medline
15. Hanrahan, J. P., Gregan, S. M., Mulsant, P., Mullen, M., Davis, G. H., Powell, R., and Galloway, S. M. (2004) Mutations in the genes for oocyte-derived growth factors GDF9 and BMP15 are associated with both increased ovulation rate and sterility in Cambridge and Belclare sheep (*Ovis aries*). *Biol. Reprod.* **70,** 900–909 CrossRef Medline
16. Belli, M., and Shimasaki, S. (2018) Molecular aspects and clinical relevance of GDF9 and BMP15 in ovarian function. in *Ovarian Cycle* (Litwack, G., ed) pp. 317–348, Elsevier Academic Press Inc., San Diego.
17. Simpson, C. M., Stanton, P. G., Walton, K. L., Chan, K. L., Ritter, L. J., Gilchrist, R. B., and Harrison, C. A. (2012) Activation of latent human GDF9 by a single residue change (Gly(391)Arg) in the mature domain. *Endocrinology* **153,** 1301–1310 CrossRef Medline
18. Al-Musawi, S. L., Walton, K. L., Heath, D., Simpson, C. M., and Harrison, C. A. (2013) Species differences in the expression and activity of bone morphogenetic protein 15. *Endocrinology* **154,** 888–899 CrossRef Medline
19. Mottershead, D. G., Sugimura, S., Al-Musawi, S. L., Li, J. J., Richani, D., White, M. A., Martin, G. A., Trotta, A. P., Ritter, L. J., Shi, J., Mueller, T. D., Harrison, C. A., and Gilchrist, R. B. (2015) Cumulin, an oocyte-secreted heterodimer of the transforming growth factor-β family, is a potent activator of granulosa cells and improves oocyte quality. *J. Biol. Chem.* **290,** 24007–24020 CrossRef Medline
20. Peng, J., Li, Q., Wigglesworth, K., Rangarajan, A., Kattamuri, C., Peterson, R. T., Eppig, J. J., Thompson, T. B., and Matzuk, M. M. (2013) Growth differentiation factor 9:bone morphogenetic protein 15 heterodimers are potent regulators of ovarian functions. *Proc. Natl. Acad. Sci. U.S.A.* **110,** E776-E785 CrossRef Medline
21. Kotzsch, A., Nickel, J., Seher, A., Sebald, W., and Müller, T. D. (2009) Crystal structure analysis reveals a spring-loaded latch as molecular mechanism for GDF-5-type I receptor specificity. *EMBO J.* **28,** 937–947 CrossRef Medline
22. Allendorph, G. P., Vale, W. W., and Choe, S. (2006) Structure of the ternary signaling complex of a TGF-β superfamily member. *Proc. Natl. Acad. Sci. U.S.A.* **103,** 7643–7648 CrossRef Medline
23. Hinck, A. P., Mueller, T. D., and Springer, T. A. (2016) Structural biology and evolution of the TGF-β family. *Cold Spring Harbor Perspect. Biol.* **8,** a022103 CrossRef
24. Goebel, E. J., Hart, K. N., McCoy, J. C., and Thompson, T. B. (2019) Structural biology of the TGF-β family. *Exp. Biol. Med.* **244,** 1530–1546 CrossRef
25. Peng, J., Wigglesworth, K., Rangarajan, A., Eppig, J. J., Thompson, T. B., and Matzuk, M. M. (2014) Amino acid 72 of mouse and human GDF9 mature domain is responsible for altered homodimer bioactivities but has subtle effects on GDF9:BMP15 heterodimer activities. *Biol. Reprod.* **91,** 142 Medline
26. Boyd, F. T., and Massagué, J. (1989) Transforming growth factor-beta inhibition of epithelial-cell proliferation linked to the expression of a 53-kDa membrane-receptor. *J. Biol. Chem.* **264,** 2272–2278 Medline

27. Attisano, L., Cárcamo, J., Ventura, F., Weis, F. M., Massagué, J., and Wrana, J. L. (1993) Identification of human activin and TGF-β type-I receptors that form heteromeric kinase complexes with type-II receptors. *Cell* **75,** 671–680 CrossRef Medline
28. Cárcamo, J., Weis, F. M., Ventura, F., Wieser, R., Wrana, J. L., Attisano, L., and Massagué, J. (1994) Type-I receptors specify growth-inhibitory and transcriptional responses to transforming growth-factor-β and activin. *Mol. Cell Biol.* **14,** 3810–3821 CrossRef Medline
29. Attisano, L., Wrana, J. L., Montalvo, E., and Massagué, J. (1996) Activation of signalling by the activin receptor complex. *Mol. Cell Biol.* **16,** 1066–1073 CrossRef Medline
30. Harrison, C. A., Gray, P. C., Koerber, S. C., Fischer, W., and Vale, W. (2003) Identification of a functional binding site for activin on the type I receptor ALK4. *J. Biol. Chem.* **278,** 21129–21135 CrossRef Medline
31. Rebbapragada, A., Benchabane, H., Wrana, J. L., Celeste, A. J., and Attisano, L. (2003) Myostatin signals through a transforming growth factor β-like signaling pathway to block adipogenesis. *Mol. Cell Biol.* **23,** 7230–7242 CrossRef Medline
32. Walker, R. G., Czepnik, M., Goebel, E. J., McCoy, J. C., Vujic, A., Cho, M., Oh, J., Aykul, S., Walton, K. L., Schang, G., Bernard, D. J., Hinck, A. P., Harrison, C. A., Martinez-Hackert, E., Wagers, A. J., Lee, R. T., and Thompson, T. B. (2017) Structural basis for potency differences between GDF8 and GDF11. *BMC Biol.* **15,** 19 CrossRef Medline
33. Li, R., Norman, R. J., Armstrong, D. T., and Gilchrist, R. B. (2000) Oocyte-secreted factor(s) determine functional differences between bovine mural granulosa cells and cumulus cells. *Biol. Reprod.* **63,** 839–845 CrossRef Medline
34. Eppig, J. J. (2001) Oocyte control of ovarian follicular development and function in mammals. *Reproduction* **122,** 829–838 CrossRef Medline
35. Russell, D. L., and Robker, R. L. (2007) Molecular mechanisms of ovulation: co-ordination through the cumulus complex. *Hum. Reprod. Update* **13,** 289–312 CrossRef Medline
36. Hussein, T. S., Thompson, J. G., and Gilchrist, R. B. (2006) Oocyte-secreted factors enhance oocyte developmental competence. *Dev. Biol.* **296,** 514–521 CrossRef Medline
37. Sudiman, J., Sutton-McDowall, M. L., Ritter, L. J., White, M. A., Mottershead, D. G., Thompson, J. G., and Gilchrist, R. B. (2014) Bone morphogenetic protein 15 in the pro-mature complex form enhances bovine oocyte developmental competence. *PLoS ONE* **9,** e103563 CrossRef Medline
38. Sugimura, S., Ritter, L. J., Sutton-McDowall, M. L., Mottershead, D. G., Thompson, J. G., and Gilchrist, R. B. (2014) Amphiregulin co-operates with bone morphogenetic protein 15 to increase bovine oocyte developmental competence: effects on gap junction-mediated metabolite supply. *Mol. Hum. Reprod.* **20,** 499–513 CrossRef Medline
39. Yeo, C. X., Gilchrist, R. B., Thompson, J. G., and Lane, M. (2008) Exogenous growth differentiation factor 9 in oocyte maturation media enhances subsequent embryo development and fetal viability in mice. *Hum. Reprod.* **23,** 67–73 Medline
40. Su, Y. Q., Sugiura, K., Li, Q., Wigglesworth, K., Matzuk, M. M., and Eppig, J. J. (2010) Mouse oocytes enable LH-induced maturation of the cumulus-oocyte complex via promoting EGF receptor-dependent signaling. *Mol. Endocrinol.* **24,** 1230–1239 CrossRef Medline
41. Nickel, J., Dreyer, M. K., Kirsch, T., and Sebald, W. (2001) The crystal structure of the BMP-2:BMPR-IA complex and the generation of BMP-2 antagonists. *J. Bone Joint Surg. Am.* **83A,** S7–S14 Medline
42. Goebel, E. J., Corpina, R. A., Hinck, C. S., Czepnik, M., Castonguay, R., Grenha, R., Boisvert, A., Miklossy, G., Fullerton, P. T., Matzuk, M. M., Idone, V. J., Economides, A. N., Kumar, R., Hinck, A. P., and Thompson, T. B. (2019) Structural characterization of an activin class ternary receptor complex reveals a third paradigm for receptor specificity. *Proc. Natl. Acad. Sci. U.S.A.* **116,** 15505–15513 CrossRef Medline
43. McKenzie, L. J., Pangas, S. A., Carson, S. A., Kovanci, E., Cisneros, P., Buster, J. E., Amato, P., and Matzuk, M. M. (2004) Human cumulus granulosa cell gene expression: a predictor of fertilization and embryo selection in women undergoing IVF. *Hum. Reprod.* **19,** 2869–2874 CrossRef Medline
44. Cillo, F., Brevini, T. A., Antonini, S., Paffoni, A., Ragni, G., and Gandolfi, F. (2007) Association between human oocyte developmental competence and expression levels of some cumulus genes. *Reproduction* **134,** 645–650 CrossRef Medline
45. Wathlet, S., Adriaenssens, T., Segers, I., Verheyen, G., Van de Velde, H., Coucke, W., Ron El, R., Devroey, P., and Smitz, J. (2011) Cumulus cell gene expression predicts better cleavage-stage embryo or blastocyst development and pregnancy for ICSI patients. *Hum. Reprod.* **26,** 1035–1051 CrossRef Medline
46. Gilchrist, R. B., Ritter, L. J., Cranfield, M., Jeffery, L. A., Amato, F., Scott, S. J., Myllymaa, S., Kaivo-Oja, N., Lankinen, H., Mottershead, D. G., Groome, N. P., and Ritvos, O. (2004) Immunoneutralization of growth differentiation factor 9 reveals it partially accounts for mouse oocyte mitogenic activity. *Biol. Reprod.* **71,** 732–739 CrossRef Medline
47. Richani, D., Constance, K., Lien, S., Agapiou, D., Stocker, W. A., Hedger, M. P., Ledger, W. L., Thompson, J. G., Robertson, D. M., Mottershead, D. G., Walton, K. L., Harrison, C. A., and Gilchrist, R. B. (2019) Cumulin and FSH cooperate to regulate inhibin B and activin B production by human granulosa-lutein cells *in vitro*. *Endocrinology* **160,** 853–862 CrossRef Medline
48. Patiño, L. C., Walton, K. L., Mueller, T. D., Johnson, K. E., Stocker, W., Richani, D., Agapiou, D., Gilchrist, R. B., Laissue, P., and Harrison, C. A. (2017) BMP15 mutations associated with primary ovarian insufficiency reduce expression, activity, or synergy with GDF9. *J. Clin. Endocrinol. Metab.* **102,** 1009–1019 Medline
49. Arnold, K., Bordoli, L., Kopp, J., and Schwede, T. (2006) The SWISS-MODEL workspace: a web-based environment for protein structure homology modelling. *Bioinformatics* **22,** 195–201 CrossRef Medline
50. Kiefer, F., Arnold, K., Künzli, M., Bordoli, L., and Schwede, T. (2009) The SWISS-MODEL Repository and associated resources. *Nucleic Acids Res.* **37,** D387–D392 CrossRef Medline
51. Nickel, J., Kotzsch, A., Sebald, W., and Mueller, T. D. (2005) A single residue of GDF-5 defines binding specificity to BMP receptor IB. *J. Mol. Biol.* **349,** 933–947 CrossRef Medline
52. Pettersen, E. F., Goddard, T. D., Huang, C. C., Couch, G. S., Greenblatt, D. M., Meng, E. C., and Ferrin, T. E. (2004) UCSF Chimera: a visualization system for exploratory research and analysis. *J. Comput. Chem.* **25,** 1605–1612 CrossRef Medline
53. Livak, K. J., and Schmittgen, T. D. (2001) Analysis of relative gene expression data using real-time quantitative PCR and the 2(T)(-$\delta\delta$C) method. *Methods* **25,** 402–408 CrossRef Medline
54. Schmittgen, T. D., and Livak, K. J. (2008) Analyzing real-time PCR data by the comparative C-T method. *Nat. Protoc.* **3,** 1101–1108 CrossRef Medline
55. Richani, D., Ritter, L. J., Thompson, J. G., and Gilchrist, R. B. (2013) Mode of oocyte maturation affects EGF-like peptide function and oocyte competence. *Mol. Hum. Reprod.* **19,** 500–509 CrossRef Medline
56. Vanderhyden, B. C., Caron, P. J., Buccione, R., and Eppig, J. J. (1990) Developmental pattern of the secretion of cumulus expansion-enabling factor by mouse oocytes and the role of oocytes in promoting granulosa-cell differentiation. *Dev. Biol.* **140,** 307–317 CrossRef Medline